

Ag/graphene Electrode for the Electrochemical Conversion of 5-Hydroxymethylfurfural to 2,5-Hexanedione at Ambient Pressure and Temperature

Maria Sarno^{a,b*}, Eleonora Ponticorvo^b

^a Department of Physics "E.R. Caianiello", University of Salerno, Via Giovanni Paolo II, 132, 84084, Fisciano (SA), Italy.

^b NanoMates, Research Centre for Nanomaterials and Nanotechnology at the University of Salerno, University of Salerno, Via Giovanni Paolo II, 132, 84084, Fisciano (SA), Italy.
 eponticorvo@unisa.it

Here we report the performance in 5-Hydroxymethylfurfural (HMF) reduction of Ag_graphene-based electrode. The prepared nanocomposite, synthesized according to a "wet chemistry" approach, was broadly characterized: SEM images and XRD spectrum indicate the formation of nanoparticles dispersed on few-layers graphene. A multimodal pore distribution, indicating a network of larger and smaller pores enabling electrode wettability and exposing surface nanoparticles, was evaluated.

The sample was tested for the oxidation of HMF in a sulfate buffer solution. A very high overpotential gap between hydrogen production and HMF conversion was demonstrated. High efficiency (FE = 65.1%) and selectivity (70.2%), with little amount of bis(hydroxymethyl)furan by-product (FE < 6%), were demonstrated.

1. Introduction

Growing concern about petroleum supply and climate change has driven the study for viable alternatives for chemical production and transportation fuels.

Biomass has emerged as a superior alternative (Rosatella et al., 2011; Huber and Dumesic, 2006; Roman-Leshkov et al., 2007) thanks to its renewable nature and the possibility of being generated through the vast number of compounds, many of which have similar or improved properties to their petroleum-based counterparts.

5-Hydroxymethylfurfural (HMF) has become one of the most crucial biomass intermediates (Lee et al., 2014). HMF can be produced from cellulosic matter, the most significant abundant organic material on earth and it can be converted into different essential chemicals (i.e. transportation fuels, polymers, pharmaceuticals...) (Peng et al., 2012).

An attractive alternative-fuel candidate is methylcyclopentane, which has a higher octane number, a higher energy content than gasoline, and low toxicity (Sacia et al., 2015). A facile and efficient route to produce methylcyclopentane is the direct conversion of 2,5-hexanedione (HD), a crucial and versatile intermediate to generate biofuels and chemicals (Sacia et al., 2015). Still, the conversion of HMF to HD (Kumalaputri et al., 2014) is achieved by the reduction of HMF by ring-opening, using expensive catalysts and hydrogen at high temperature and pressure.

The electrochemical approach (Sarno et al., 2019a, Sarno and Ponticorvo, 2019), which requires non-extreme reaction conditions, is a valid alternative. For electrochemical reduction of HMF in aqueous media, H₂ generation is the primary competing reaction (You B., 2016). Therefore, the combination of a performing HMF reduction and poor hydrogen evolution reaction (HER) catalyst is needed for achieving high Faradaic efficiency (FE) for HMF reduction.

In this study, Ag_graphene nanocomposite was synthesized and characterized by the combined use of different techniques. The direct electrochemical conversion of HMF to HD at ambient pressure and temperature was demonstrated in a sulfate buffer solution in a conventional three-electrode cell (Sarno and Ponticorvo, 2017). Water was used as the hydrogen source and Ag_graphene nanocomposite as the catalytic

electrode. The catalyst, which consists of a low amount Ag nanoparticles, exhibiting weak H₂ evolution catalysis (Back et al., 2015), stabilized on a conductive graphene sheet (Sarno and Ponticorvo, 2018; Singh et al., 2012), was used for HMF reduction. High HMF conversion and electrode durability were demonstrated.

2. Experimental Section

2.1 Nanocomposite synthesis

Silver nitrate (1 mmol) and few-layer graphene (0.25 g) were loaded into the reagent mixture, consisting of 20 ml of 1-octadecene, oleic acid (6 mmol), oleylamine (6 mmol) and 1,2-hexadecandiol (10 mmol) as reducing agent. The temperature was increased to 200 °C for 2 h and then the mixture was heated up to 285 °C for 1 h, in inert ambient (Sarno et al., 2015; Sarno et al., 2016a; Sarno et al., 2017). After synthesis had occurred, Ag-graphene nanocomposite obtained were purified alternating ethanol and hexane washing and separated by centrifugation (Sarno et al., 2019b). To remove the organic content, thermal treatment at 150 °C for 8h followed.

2.2 Characterization methods

Bruker D8 X-ray diffractometer was used for X-ray diffraction spectroscopy. Scanning electron microscopy (SEM) was performed through the use of an LEO 1525 electron microscope. N₂ adsorption-desorption (Kelvin 1042 V3.12, COSTECH Instruments) at 77 K makes it possible to determine the surface area, after 250 °C for 3 h pretreatment in He (Ciambelli et al., 2004). Electrochemical measurements were performed employing the Autolab PGSTAT302N potentiostat/galvanostat. To obtain the electrodes, 4 mg of synthesized nanocomposites were dispersed into 80 µl of a 5 wt% Nafion solution, 200 µl of ethanol and 800 µL of distilled water. HMF electrochemical conversion was evaluated in a three-electrode batch cell through linear voltammetry (LV) experiments at 20 mV/s in sulfate buffer solution (Figure 1).

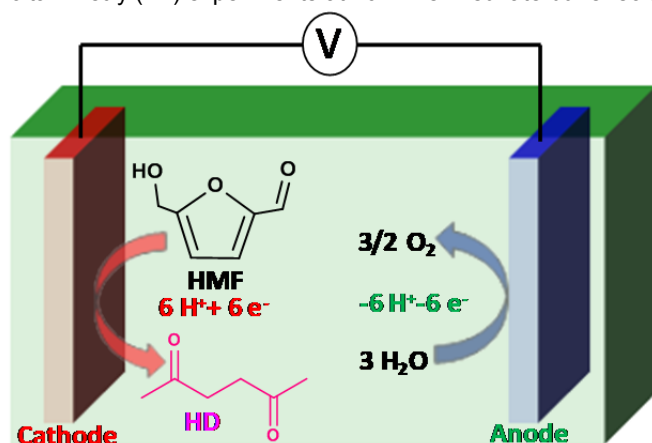


Figure 1: Representation of HMF electrochemical conversion.

The electrocatalyst performance was also evaluated in the absence of HMF. Nitrogen was supplied continuously to the cell. ¹H NMR analyses of reaction products were performed using Bruker Advance 400 (Operating at 400 MHz), deuterated chloroform (CDCl₃) was used for the measurements.

3. Results and discussion

3.1 Ag_graphene nanocomposite characterization

In Figure 2 The X-ray diffraction pattern of Ag_graphene nanocomposite is shown. In particular, the typical peaks of silver are visible, i.e. peaks at 38.5° (111), 44.6° (200), 65.1° (220), 77.71° (311) can be detected (Anandalakshmi et al., 2016). The Ag crystalline size measured by Scherrer's equation (Sarno et al., 2014; Sarno et al., 2016b) was found to be 25 ± 0.5 nm (applied on the (111) peak).

SEM measurements (Figure 3) were performed to evaluate the layers' size of graphene nanosheets. The nanocomposite resulted constituted of layers varying from one micrometer to about two micrometers (Zhou et al., 2018; Sarno et al., 2019c). Ag nanoparticles dispersed, almost homogeneously, on graphene sheets are also visible.

The Ag particle size distribution, obtained from a statistical analysis of over 150 nanoparticles, shown in Figure 4, highlights that the average diameter is 26.2 nm with a standard deviation of 5.02 nm.

The BET surface area for Ag_graphene nanocomposite obtained from N₂ adsorption-desorption analysis was found equal to 89.11 m²/g. The distribution is a multimodal, BJH (Barrett-Joyner-Halenda) pore distribution, centered at 2.7, 6.2, 9.4, and 30.1 nm, indicating a network of larger and smaller pores enabling electrode wettability and exposing nanoparticles surface.

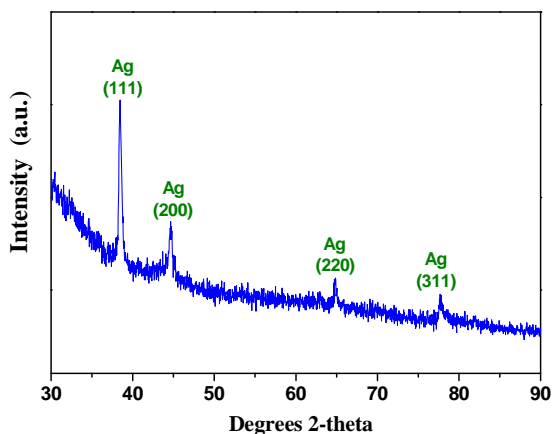


Figure 2: XRD spectrum of Ag_graphene nanocomposite.

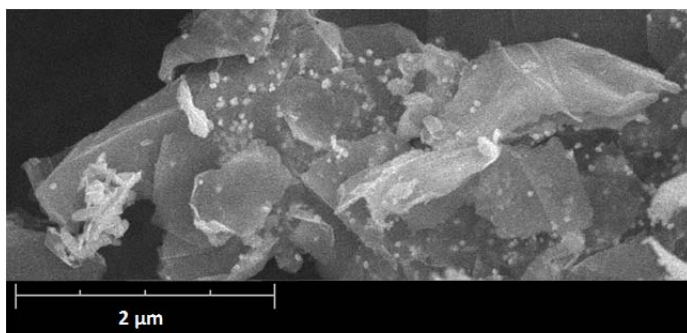


Figure 3: SEM image of Ag_graphene nanocomposite.

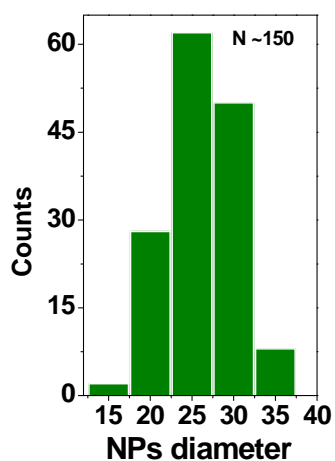


Figure 4: size distribution histogram of Ag_graphene nanocomposite.

3.2 HMF electrochemical conversion

For electrochemical reduction of HMF in aqueous media, hydrogen evolution reaction is the primary competing reaction. Finding active and performing HMF reduction catalysts among electrochemically active catalysts, but weak H_2 evolution promoting, is needed for obtaining high HMF reduction Faradaic efficiency (FE). Ag was selected as poor H_2 evolution catalysts and graphene as conductive support. Linear voltammetry (LV) was obtained in a 0.2 M sulfate buffer solution (pH 2.0) (Figure 5). The cathodic currents in LVs profile, acquired in the absence of HMF, are generated as a result of the reaction of hydrogen production. A high HER overpotential was observed (~ 0.5 V). When the Ag_graphene electrode was used, in the presence of HMF (Figure 5, dot line), the reduction overpotential shifted in a positive direction (high shift of 300 mV), suggesting that HMF conversion takes place before H_2 production. On the other hand, when HMF was added, Pt catalyst alone, not shown here, did not display a change both in the overpotential and in the cathodic current curve. This is because H_2 evolution predominates on the Pt electrode, and no HD was detected.

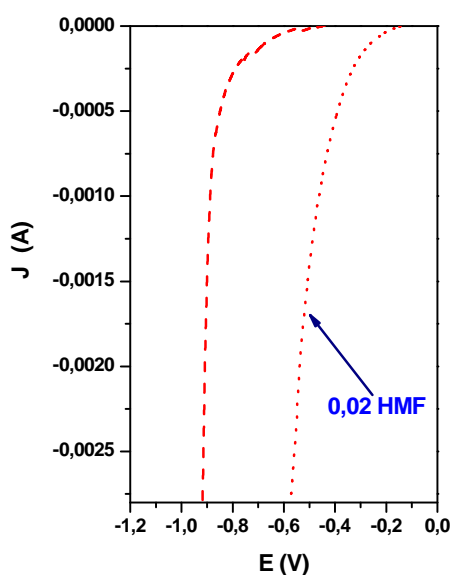


Figure 5: LSVs of Ag_graphene nanocomposite in 0.2 M sulfate buffer solution with and without 0.02 M HMF. A scan rate of 20 mV/s.

The calculated Tafel slope little increased from 79 mV/dec to 85 mV/dec (Figure 6) after the addition of HMF in the sulfate buffer solution, indicating a high HMF conversion rate. Also, chronopotentiometry recorded for six hours experiment conducted at a current density of 3×10^{-4} A with 0.02 M HMF showed that the required potential is stable during the test time. The small fluctuation is due to the formation and release of bubbles on the catalyst surface.

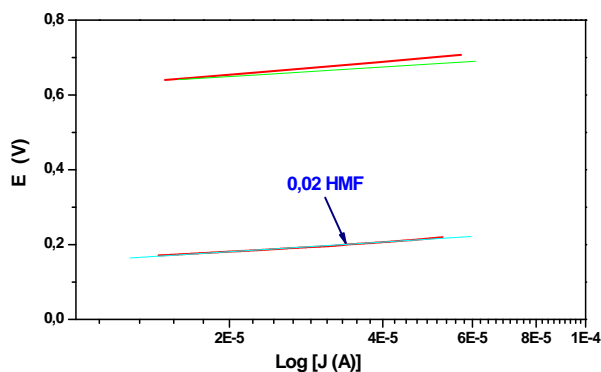


Figure 6: Tafel plots of Ag_graphene nanocomposite in 0.2 M sulfate buffer solution with and without 0.02 M HMF. A scan rate of 20 mV/s.

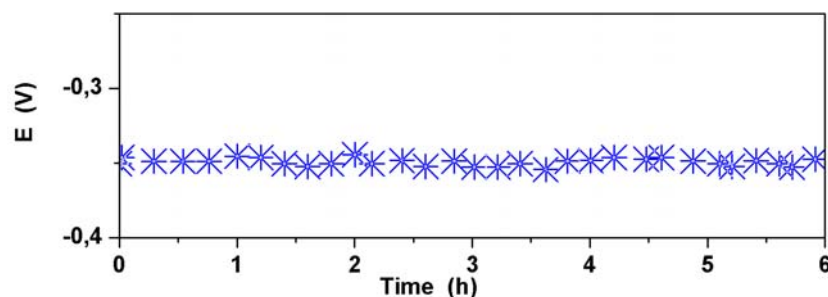


Figure 7: Chronopotentiometric profile of Ag_graphene nanocomposite in 0.2 M sulfate buffer solution with 0.02 M HMF.

After reduction, the reaction medium was collected and analyzed by $^1\text{H-NMR}$ to quantify the products. FE and selectivity for HD generation were evaluated through the following equations:

$$\text{FE}(\%) = \frac{\text{HD (mol) produced}}{C/(F \cdot n)} * 100\% \quad (1)$$

$$\text{selectivity}(\%) = \frac{\text{HD (mol) produced}}{\text{HMF (mol) converted}} * 100\% \quad (2)$$

Where F is the Faraday constant and n is the number of electrons required (equal to 6) for the of HMF to HD conversion. Using a Pt electrode, a trivial amount of HMF was converted, with the FE of 2.3% for 2,5-bis(hydroxymethyl)furan (BHMF) generation. On the other hand, the Ag_graphene electrode produced HD with high efficiency (FE = 65.1%) and selectivity (70.2%), and a small amount of BHMF (FE < 6%) was detected.

The highest FE was achieved at -0.5 V . On the other hand, applying a more negative voltage, a reduction of FE was observed, indicating that HER became more favorable in the high overpotential region. When a higher potential was chosen, the average cathodic current decreased, indicating a reduction of HD production rate.

4. Conclusions

In summary, a simple and efficient strategy was applied to synthesize an Ag_graphene based electrode. XRD and SEM analysis confirmed the formation of the nanocomposite as mentioned above structure.

The prepared nanocomposite has been tested as an electrochemical catalyst in order to reduce HMF in sulfate buffer solutions, to give HD at the cathode. It occurs at lower potentials (0.2 V) than required for hydrogen evolution.

Further studies will be focused on the collection and quantification of HD produced in a two compartments cell (Membrane Electrode Assembly (MEA) apparatus). In this case, simultaneously the conversion of HMF, to give pure HD, and, at the counter electrode, the production of oxygen gas, should be favored.

References

- Anandalakshmi K., Venugobal J., Ramasamy V., 2016, Characterization of silver nanoparticles by green synthesis method using *Pedaliium murex* leaf extract and their antibacterial activity, Applied Nanoscience, 6, 399-408.
- Back S., Yeom M.S., Jung Y., 2015, Active Sites of Au and Ag Nanoparticle Catalysts for CO₂ Electroreduction to CO, ACS Catalysis, 5, 5089-5096.
- Ciambelli P., Sannino D., Sarno M., Fonseca A., Nagy J.B., 2004, Hydrocarbon decomposition in alumina membrane: An effective way to produce carbon nanotubes bundles, Journal of Nanoscience and Nanotechnology, 4, 779-787.
- Huber G.W., Dumesic J.A., 2006, An Overview of Aqueous-Phase Catalytic Processes for Production of Hydrogen and Alkanes in a Biorefinery, Catalysis Today, 111, 119-132.

- Kumalaputri A.J., Bottari G., Erne P.M., Heeres H.J., Barta K., 2014, Tunable and Selective Conversion of 5-HMF to 2,5-Furandimethanol and 2,5-Dimethylfuran over Copper-Doped Porous Metal Oxides, *ChemSusChem*, 7, 2266-2275.
- Lee Y.-C., Dutta S., Wu K.C.-W., 2014, Integrated, Cascading Enzyme-/Chemocatalytic Cellulose Conversion using Catalysts based on Mesoporous Silica Nanoparticles, *ChemSusChem*, 7, 3241-3246.
- Peng W.-H., Lee Y.-Y., Wu C., Wu K. C.-W., 2012, Acid–base bi-functionalized, large-pored mesoporous silicananoparticles for cooperative catalysis of one-pot cellulose-to-HMF conversion, *Journal of Materials Chemistry*, 22, 23181-23185.
- Roman-Leshkov Y., Barrett C. J., Liu Z.Y., Dumesic J.A., 2007, Production of dimethylfuran for liquid fuels from biomass-derived carbohydrates, *Nature*, 447, 982-986.
- Rosatella A.A., Simeonov S.P., Frade R.F.M., Afonso C.A.M., 2011, 5-Hydroxymethylfurfural (HMF) as a building block platform: Biological properties, synthesis and synthetic applications, *Green Chemistry*, 13, 754-793.
- Sacia E., Deaner M., Louio Y., Bell A., 2015, Synthesis of biomass-derived methylcyclopentane as a gasoline additive via aldol condensation/hydrodeoxygenation of 2,5-hexanedione, *Green Chemistry*, 17, 2393-2397.
- Sarno M., Cirillo C., Ciambelli P., 2014, Selective graphene covering of monodispersed magnetic nanoparticles, *Chemical Engineering Journal*, 246, 27–38.
- Sarno M., Cirillo C., Ponticorvo E., Ciambelli P., 2015, Synthesis and Characterization of FLG/Fe₃O₄ Nanohybrid Supercapacitor, *Chemical Engineering Transactions*, 43, 943-948.
- Sarno M., Cirillo C., Scudieri C., Polichetti M., Ciambelli P., 2016b, Electrochemical Applications of Magnetic Core–Shell Graphene-Coated FeCo Nanoparticles, *Industrial and Engineering Chemistry Research*, 55, 3157-3166.
- Sarno M., Iuliano M., Polichetti M., Ciambelli P., 2017, High activity and selectivity immobilized lipase on Fe₃O₄ nanoparticles for banana flavour synthesis, *Process Biochemistry*, 56, 98-108.
- Sarno M., Ponticorvo E., 2018, Cu-graphene nanostructures for low concentration CH₃SH removal, *Chemical Engineering Transactions*, 68, 487-492.
- Sarno M., Ponticorvo E., 2019, Metal–metal oxide nanostructure supported on graphene oxide as a multifunctional electro-catalyst for simultaneous detection of hydrazine and hydroxylamine, *Electroly Communications*, 107, 106510.
- Sarno M., Ponticorvo E., Cirillo C., Ciambelli P., 2016a, Magnetic nanoparticles for PAHs solid phase extraction. *Chemical Engineering Transactions*, 47, 313–318.
- Sarno M., Ponticorvo E., Scarpa D., 2019a, Controlled PtIr nanoalloy as an electro-oxidation platform for methanol reaction and ammonia detection, *Nanotechnology*, 30, 394004.
- Sarno M., Ponticorvo E., Scarpa D., 2019b, PtRh and PtRh/MoS₂ nano-electrocatalysts for methanol oxidation and hydrogen evolution reactions, *Chemical Engineering Journal*, 377, 120600.
- Sarno M., Ponticorvo E., Scarpa D., 2019c, Ru and Os based new electrode for electrochemical flow supercapacitors, *Chemical Engineering Journal*, 377, 120050.
- Sarno M., Ponticorvo E., 2017, Much enhanced electrocatalysis of Pt/PtO₂ and low platinum loading Pt/PtO₂-Fe₃O₄ dumbbell nanoparticles, *International Journal of Hydrogen Energy*, 42, 23631-23638.
- Singh M.K., Titus E., Krishna R., Goncalves G., Marques P.A.A.P., Gracio J., 2012, Direct Nucleation of Silver Nanoparticles on Graphene Sheet, *Journal of Nanoscience and Nanotechnology*, 12, 1-6.
- You B., Liu X., Jiang N., Sun Y., 2016, General Strategy for Decoupled Hydrogen Production from Water Splitting by Integrating Oxidative Biomass Valorization, *Journal of the American Chemical Society*, 138, 13639-13646.
- Zhou L., Fox L., Włoddek M., Islas L., Slastanova A., Robles E., Bikondoa O., Harniman R., Fox N., Cattelan M., Briscoe W.H., 2018, Surface structure of few layer graphene, *Carbon*, 2018, 136, 255-261.